RASĀYAN *J. Chem.*
Vol. 18 | No. 1 |412-421| January - March | 2025
ISSN: 0974-1496 | e-ISSN: 0976-0083 | CODEN: RJCABP
http://www.rasayanjournal.com
http://www.rasayanjournal.co.in

STUDY OF BIOCORROSION MITIGATION OF MILD STEEL USING TRIAZOLE DERIVATIVE

Dhanali Shah✉ and R. S. Dubey
Chemistry Research Laboratory, Department of Chemistry, R.J College (Autonomous),
Affiliated to the University of Mumbai, Ghatkopar (W), Mumbai-400086, India.
✉Corresponding author: dhanalishah1004@gmail.com

ABSTRACT

In the present study, N-((1H-benzo[d]1,2,3]traizol-1-yl)methyl)-4-chlorobenzenamine a synthesized derivative of benzotriazole was selected for evaluating its corrosion protective property on mild steel exposed to sulfate-reducing bacteria (*Desulfovibrio desulfuricans)*. The anti-corrosive property was studied with a preliminary experiment named gravimetric analysis with concentrations ranging from 100 ppm to 500 ppm, and electrochemical techniques like open circuit potential and potentiodynamic polarization were studied. As per the results obtained, the compound works out to be an efficient corrosion-protecting agent against the production of biogenic H_2S, with an inhibition efficiency of 85.0% to 86.66% at 500 ppm concentration. The decrease in efficiency was observed after 216 hrs. The surface morphology was obtained from bio-corroded MS coupons with and without inhibitor with scanning electron microscopy and the composition of MS surfaces was analyzed with Energy dispersive x-ray analysis technique. The acquired data precisely followed Langmuir Adsorption Isotherm. Evaluating the results obtained, the inhibitor showed both physisorption and chemisorption, forming a barrier between the MS surface and a corrosive environment with SRB.

Keywords: Biocorrosion, Mild steel, *Desulfovibrio desulfuricans*, Benzotriazole, Biocide, Anti-Corrosive
RASĀYAN*J. Chem.*, Vol. 18, No.1, 2025

INTRODUCTION

The attack on a metal surface that acts as a substrate for a wide range of micro-organisms that disturb the mechanical and chemical properties through electrochemical reaction is called microbiologically influenced corrosion (MIC).[1-4] Mild steel possesses good physical and mechanical properties and is used in cooling water systems for pipeline structures. MIC is usually associated with pitting type and localized form of corrosion which is more harmful to the metal structure causing high economic loss. A single species of organism is not responsible for the bio-corrosion but the presence of consortia of organisms taking part in the reaction at different stages. The main culprit of corrosion in an anoxic environment is the growth of sulfate-reducing bacteria (SRB), which uses elemental sulfur and sulfur compounds as terminal electron acceptors for the growth which results in sour corrosion i.e. production of H_2S, which speeds up the ion dissolution. The main product of bio-corrosion due to SRB is sulphide.[4,11] SRB found in damaged areas enter into the system via natural habitation like seawater used in cooling water systems, pipelines buried in soil, etc. SRB grows in oxygen-depleted zones where the condition of fluid is stagnant for a longer period or low velocity of the fluid, organic molecules are oxidized to yield energy and sulfur acts as a terminal electron acceptor. As the conditions get favorable, eventually the formation of biofilm takes place at the lower parts where the planktonic cells get attached to the surface secreting extracellular polymeric substances (EPS), new young cells are formed and older cells mature releasing out the newer young cells and the older cells stay at the base.[5-8] MIC cannot be completely desisted but can be slowed. Different classes of organic compounds having both biocidal or biostatic and anti-corrosive properties, organic molecules like triazine, azoles, quinolines, etc. are used due to the presence of hetero-atoms in the ring structure. Heterocyclic compounds are usually used against corrosion as they have been proven to have effective corrosion inhibition efficiency. The conjugated system and the hetero atoms like nitrogen, sulfur, and oxygen boost the adsorption process on the metal surface. The position of delocalized pi-electrons and conjugate system governs the adsorption process on the metal substrate. The adsorption takes place between the unoccupied d-orbital of the metal iron and the lone pair of electrons.[12,13] Triazole is made of aromatic compounds of benzene and triazole ring fused making it a bicycling ring moiety. Triazole and its derivatives

http://doi.org/10.31788/RJC.2025.1819178
This work is licensed under a CC BY 4.0 license.

have a wider range of applications in anti-corrosive, anti-inflammatory, anti-tumor, and against a wide class of pathogenic organisms and so on.[9-11] In the present study, benzotriazole derivative was synthesized and used as a mitigating agent against the biocorrosion activity of SRB namely *Desulfovibrio desulfuricans*. To get the measure of corrosion inhibition of MS, gravimetric analysis at various concentrations of inhibitor was carried out. Electrochemical analysis namely open circuit potential (OCP) and potentiodynamic polarization (PD), surface characterization was evaluated with Scanning Electron Microscopy, and Energy dispersive x-ray for coupons with and without inhibitor was carried out.

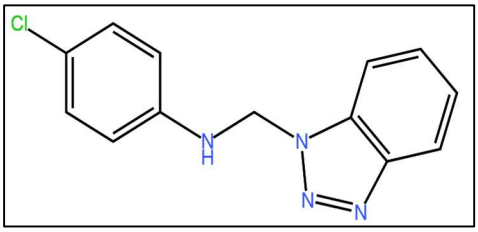

Fig.-1: Molecular Structure of N-((1H-benzo[d]1,2,3] traizol-1-yl)methyl)-4-chlorobenzenamine

EXPERIMENTAL

Organisms and Culture Media

The bacterial culture taken into consideration was *Desulfovibrio desulfuricans* (NCIM No - 2047) obtained from the National Collection of Industrial Microorganisms (NCIM), Biochemical Science Division, National Chemical Laboratory, Pune- 411088, Maharashtra. Barr's media was used for the growth and enrichment of bacterial culture having media composition as follows:

Components and quantity in grams: K_2HPO_4 0.05g, NH_4Cl 0.19g, $CaSO_4$ 0.29g, sodium Lactate 0.79g, $MgSO_4.7H_2O$ 0.29g, $Fe(NH_4)_2(SO_4)_2$ 0.05g, Distilled water 100cm^3.

The media was sterilized for three consecutive days at 121°C for 15 - 20 min, after every autoclave pH was adjusted to 7.0-7.5 and the final pH of the media was 7.0 - 7.5.

Preparation of Metal Coupons

Mild Steel coupons composed of C-0.16%, Si-0.10%, Mn-0.40%, P-0.013%, S-0.02%, and remaining iron, were used as a working electrode. These coupons had dimensions of 3.5 cm*1.0cm*0.02 cm of rectangular shape. Coupons were polished with emery paper no. 60, 80, 100, 120, 150 and 180. They were washed with double distilled water, rinsed with acetone, disinfected with ethanol, and dried in a desiccator.

Synthesis of Anti-Corrosive Agent

STEP 1Synthesis of 1-(chloromethyl)-1-H-benzo [1,2,3] Triazole

Benzotriazole (0.02 mol), and dichloromethane (0.1 mol) were dissolved in 20 ml of DMF. Potassium carbonate (0.02 mol) was mixed and refluxed for 6 hrs. The crude product was obtained by adding ice-cold water to the reaction mixture.

STEP 2 Synthesis of N-((1H-benzo[d]1,2,3] traizol-1-yl) methyl)-4-chlorobenznamine

The crude obtained from step 1 was further reacted with 4-chloroaniline (substituted aniline) in DMF and refluxed for 6 hrs. The final residue was obtained by adding ice-cold water to get the desired derivative**.**

The product obtained was filtered, and vacuum dried. Recrystallization of the obtained final crude product was carried out using ethanol.[14]

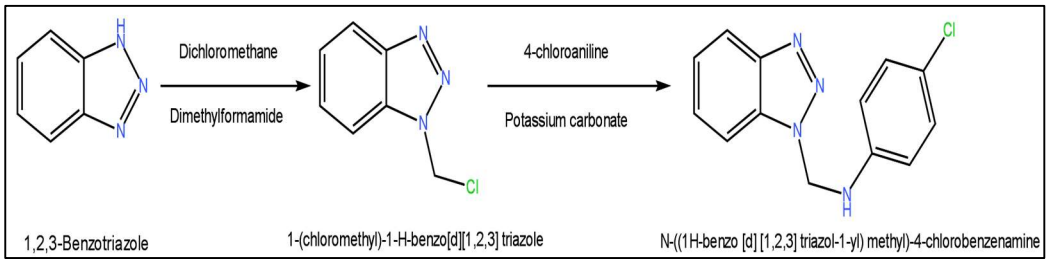

Fig.-2: Synthesis of N-((1H-benzo[d]1,2,3] traizol-1-yl) methyl)-4-chlorobenzenamine

Weight Loss Method

The test for bio-corrosion was initially evaluated by gravimetric analysis. Mild steel coupons were polished with emery paper no 60,80,100,120,150 and 180, further washed with double distilled water, rinsed with acetone disinfected with ethanol, dried, and stored. The weight of these test coupons was noted before immersing them in Barr's Media with test culture (corrosive media) and varying concentrations of the inhibitor. Weight changes were observed after 96 hours, 216 hours, and 312 hours respectively at room temperatures. The corrosion rate was calculated using Eq (1).

$$CR = \frac{w}{S.t} \quad (1)$$

Where CR stands for corrosion rate, w is the difference between the initial weight and final weight of coupons immersed, s counts for the surface area of the rectangular MS coupons immersed, and t is the time of immersion in hours.

The efficiency of the inhibitor against bio-corrosion was calculated as per the given formula, Eq (2).

$$\text{IE (\%)} = \frac{CR-CR\prime}{CR} \times 100 \quad (2)$$

Where, IE: corrosion inhibition efficiency, CR and CR': rate of corrosion without inhibitor and with inhibitor respectively.

Electrochemical Analysis

Electrochemical analysis naming open circuit potential (OCP) and potentiodynamic polarization (PD) was experimented on Squidstat Solo Instrument series no 2181 and analyzed on Admiral software. Using enamel lacquer 1cm^2 polished mild steel coupon was masked keeping a tiny passage for the current to follow, and was used to carry out open circuit potential (OCP) and potentiodynamic polarization (PD) techniques. A Pyrex three-necked glass electrode vessel was used with a working electrode as mild steel coupons sat. Calomel electrode as standard electrode and graphite as an auxiliary electrode. These electrodes were immersed in Barr's media having test culture and inhibitor. Squidstat Solo Instrument was connected to the respective electrodes. The potentials obtained were swept between -250mV to +250mV at a scan rate of 5 mV/s. The open circuit potentials (OCP) were carried out for sixty minutes to obtain a steady curve. Then potentiodynamic polarization (PD) curves were obtained for mild steel coupons.

Surface Analysis

Morphology of mild steel surface for corroded and non-corroded coupons after immersion in Barr's media with bacterial culture with inhibitor and without inhibitor was analyzed with Scanning Electron Microscopy (SEM) and its surface composition was analyzed with Energy dispersive x-ray analysis (EDAX).

RESULTS AND DISCUSSION

Characteristics of N-((1H-benzo[d]1,2,3] traizol-1-yl) methyl)-4-chlorobenznamine

Characterization of the synthesized test inhibitor was carried out with 'Fourier Transform Infrared Spectrum (FTIR)' in the range of 500-4000 cm-1 at a resolution of 2 cm^{-1} using the Perkin-Elmer 1710 spectrophotometer. Yield: 52%, FTIR: 3016.18 cm^{-1} (Ar-H stretching), 3348.19 cm^{-1}(NH Stretching), 3363.62 cm^{-1}(N-N stretching), 1342.36 cm^{-1}(C=N Stretching), 2268.13 cm^{-1}(N-C Stretching), 794.62 cm^{-1}(C-Cl bending).

Weight Loss Measurements

Effect of N-((1H-benzo[d]1,2,3] triazole-1-yl) methyl)-4-chlorobenzenamine

Corrosion inhibition of MS in a corrosive bacterial environment for concentrations ranging from 100 ppm to 500 ppm solutions is listed in Table-1. As per the results obtained, an increase in inhibition efficiency and a decrease in corrosion rate was observed respectively with an increase in inhibitor concentration. The heterocyclic compound forms a barrier between the MS surface area and the corrosion environment which shows the presence of planktonic cells in the environment. This barrier is formed as there is adsorption of inhibitors on the surface area thereby blocking the active area where the cells tend to attack.[15,16]

Table-1: Inhibition Efficiency and Corrosion Rate of Mild Steel Coupons without and with inhibitor at Room Temperature for 216 hrs.

S. No.	Concentration (ppm)	$w_1 - w_2$ (mg)	Surface coverage (ɵ)	Inhibition Efficiency (%)	Corrosion Rate ($mgcm^{-2}h^{-1}$)
1	Blank	20	--	--	0.0128
2	100	11	0.45	45.00	0.0071
3	200	8	0.60	60.00	0.0051
4	300	5	0.75	75.00	0.0032
5	400	4	0.80	80.00	0.0025
6	500	3	0.85	85.00	0.0019

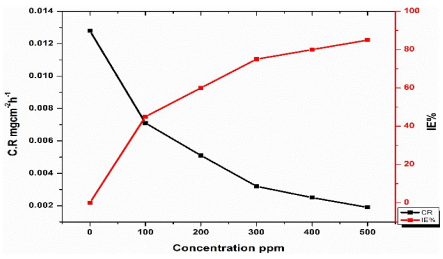

Fig.-3: Co-relation between Concentration of Inhibitor, Inhibition Efficiency, and Corrosion Rate at 216 hrs

The factors affecting the adsorption of N-((1H-benzo[d]1,2,3] traizol-1-yl) methyl)-4-chlorobenzenamine molecule on the surface of MS are the presence of hetero-atom like N, conjugated system, delocalized pi-electrons and benzotriazole molecule. As per Table (1), the corrosion rate decreased from 0.0128 mg $cm^{-2}h^{-1}$ to 0.0019 mg $cm^{-2}h^{-1}$ for counter to 500 ppm solution respectively. The highest inhibition efficiency of 85.00% was observed for 500 ppm solution. Fig (3), represents the relation between the concentrations of inhibitor, inhibition efficiency, and corrosion rate respectively. This decrease and increase in corrosion rate and inhibition efficiency respectively, were due to inhibitors covering the active sites on the surface of metal to protect biofilm formation.[19]

Effect of Incubation Time on MS Coupons

Gravimetric data after 96 hours and 312 hours was noted along with 216 hours to find out the most effective inhibition efficiency. Table (2), gives the data of corrosion rate and inhibition efficiency at 96 hours, as the concentration increases the decrease in corrosion rate and increase in inhibition efficiency was seen respectively, with a maximum IE% of 86.66 at 500 ppm solution.

Table-2: Inhibition Efficiency and Corrosion Rate of Mild Steel Coupons without and without Inhibitor at Room Temperature for 96 hours

S. No.	Concentration (ppm)	$w_1 - w_2$ (mg)	Surface coverage (ɵ)	Inhibition Efficiency (%)	Corrosion Rate ($mgcm^{-2}h^{-1}$)
1	Blank	15	--	--	0.0217
2	100	8	0.46	46.66	0.0116
3	200	7	0.5333	53.33	0.0101
4	300	5	0.6666	66.66	0.0072
5	400	4	0.7333	73.33	0.0058
6	500	2	0.8666	86.66	0.0029

Table-3, shows that the corrosion rate decreases with an increase in concentration and increase in inhibition efficiency increases respectively, at 312 hours. Maximum efficiency was observed to be 62.02% at a 500ppm concentration of inhibitor. Comparing the weight loss data obtained at different time (hrs) intervals, it was observed that maximum inhibition efficiencies were noted at 216 hours as compared to 96 hours and 312 hours. After 216 hours, the decrease in inhibition efficiency and increase in corrosion rate was noted, this may be due to a break or crack that leads to denaturation of the protective film on the metal surface which stimulated the metal interaction with the corrosive environment and resulted in corrosion.[17,23] The correlation between corrosion rate and inhibition efficiency is shown in Fig. 4(a) and 4(b) after 96 hours and 312 hours respectively.

Table-3: Inhibition Efficiency and Corrosion Rate of Mild Steel Coupons Without and without Inhibitor at Room Temperature for 312 Hours

S.No.	Concentration (ppm)	$w_1 - w_2$ (mg)	Surface coverage (ϴ)	Inhibition Efficiency (%)	Corrosion Rate ($mgcm^{-2}h^{-1}$)
1	Blank	29	--	--	0.0129
2	100	21	0.2758	27.58	0.0093
3	200	18	0.3793	37.93	0.0080
4	300	15	0.4482	44.82	0.0066
5	400	12	0.5862	58.62	0.0053
6	500	10	0.6206	62.02	0.0044

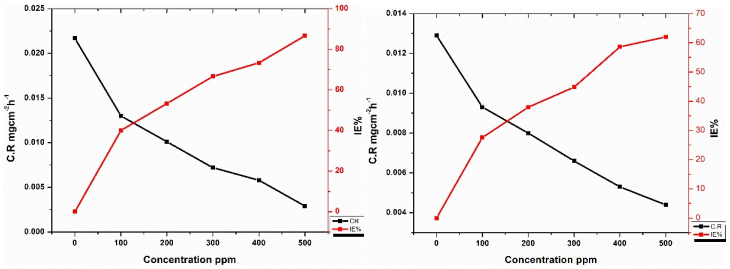

Fig.-4(a) Fig.-4(b)

Fig.-4: Correlation between Concentration of Inhibitor, Inhibition Efficiency, and Corrosion Rate at (a) 96 Hours and (b) 312 Hours

Adsorption Isotherms

Most organic inhibitors show adsorption mechanisms to occupy the active sites on MS coupons. Adsorption Isotherms show an interaction between the MS surface and the biocide i.e. corrosion inhibitor. Various adsorption isotherms like Langmuir, Freundlich, Temkin, and so on were plotted to give the best-fitted graph for the following data of surface coverage and the concentration of inhibitor in molarity. Amongst these, Langmuir adsorption isotherms have fitted precisely for the calculated data with Eq. (3).

$$\frac{C}{\theta} = \frac{1}{k_{ads}} + c \qquad (3)$$

Where C is the concentration of the organic compound as Inhibitor, (K_{ads}) is the adsorptive equilibrium constant, and (θ) is the surface coverage. It is calculated as

$$\theta = \frac{CR - C'}{CR} \qquad (4)$$

Where, CR and CR' is the corrosion rates of the counter and for anti-corrosive agent for respective concentrations. Fig. 4(a) and 4 (b) is the plot of C/θ vs. C showing linear coefficient regression(R^2) values which were close to unity and the slope, indicating it follows Langmuir adsorption isotherms, resulting in the formation of a monolayer of inhibitor on the MS surface. K_{ads} values show the strength by which the inhibitor gets adsorbed on the metal surface.[18] Table-4 shows the values of (K_{ads}) for N-((1H-benzo[d]1,2,3] traizol-1-yl) methyl)-4-chlorobenzenamine for varying time. The values of K_{ads} were obtained from the plot of C/θVs C. ΔG^0_{ads} is the standard free energy one of the thermodynamic parameters calculated from Eq (5) and (6)

$$K_{ads} = \frac{1}{55{\cdot}5} exp\ exp\left[-\frac{\Delta G^0_{ads}}{RT}\right] \qquad (5)$$

$$\Delta G^0_{ads} = \Delta H^0_{ad} - T\Delta S^0_{ads} \qquad (6)$$

Where ΔG^0_{ads} is the standard free energy, k_{ads} is the adsorption equilibrium constant, R is the universal gas constant, T is the thermodynamic temperature and a value of 55.5 is the molar concentration of water in solution.ΔG^0_{ads} gives us information on whether the inhibition shows physisorption or chemisorption with metal surfaces. If the values of ΔG^0_{ads} is greater than -20kJmol^{-1} there is physical adsorption taking place and if the value is greater than -40kJmol^{-1} is chemisorption. In the case of physisorption, it is the electrostatic interaction between charged species that provides a lone pair of electrons of the inhibitor molecule and the

iron surface providing the vacant d-orbital, whereas for chemisorption it is the interaction between the charged portion of the inhibitor and the metal surface where there is covalent formation respectively. Table (4) shows the values obtained where k_{ads} are -28.709 kJ/mol, -29.154 kJ/mol and -27.060 kJ/mol which states that it is both physisorption and chemisorption.[19,20]

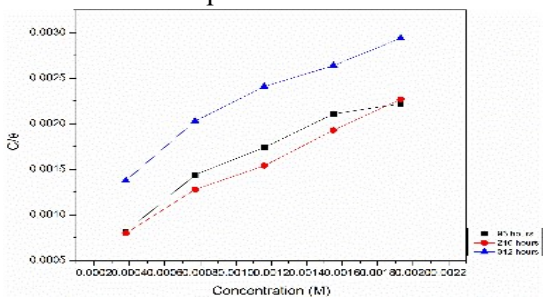

Fig.-5: Langmuir Adsorption Isotherm of Mild Steel Understudy at 96 Hours, 216 Hours, and 312 Hours

Table-4: Thermodynamic Parameters of N-((1H-benzo[d]1,2,3] traizol-1-yl) methyl)-4-chlorobenzenamine at Different Time Interval

S. No.	Incubation time (hours)	R^2	Slope	K_{ads}	$-\Delta G^0_{ads}$ KJ/mol
01	96	0.945	0.901	1603.53	28.709
02	216	0.995	0.908	1913.67	29.154
03	312	0.957	0.957	833.33	27.060

Electrochemical Analysis

Open circuit potential measurement

Figure-6, the graphs obtained from open circuit potential for MS coupons with inhibitor for concentrations ranging from 100 ppm to 500 ppm solution with SRB inoculated and for counter MS coupons without inhibitor with SRB. The graph obtained shows the shift of potential towards the positive side as compared to MS coupons without inhibitors. As there is a positive shift presence of N-((1H-benzo[d]1,2,3]traizol-1-yl) methyl)-4-chlorobenzenamine molecules, suggesting the impact is on the anodic part of the reaction on MS. In addition to this, the more the concentration of the inhibitor, the potential has shifted towards a more positive terminal. This also indicates the inhibitor is getting more adsorbed on the MS plate.[22]

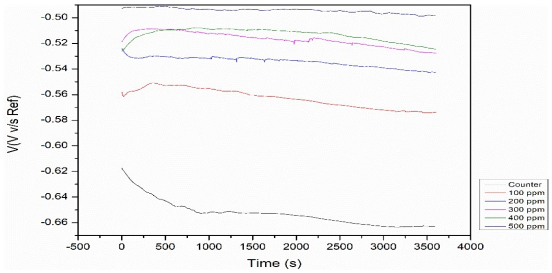

Fig.-6: Open Circuit Potential (OCP) Graphs of MS in Barr's Media Inoculated SRB and with Varying Concentrations of N-((1H-benzo[d]1,2,3] traizol-1-yl) methyl)-4-chlorobenzenamine

Polarization Measurements

Polarization curves were recorded for MS in the presence and absence of inhibitor N-((1H-benzo[d]1,2,3] traizol-1-yl) methyl)-4-chlorobenzenamine was obtained for varying concentrations. Figure-7 shows the polarization curve obtained respectively. Table (5), lists the electrochemical kinetic parameters like (E_{corr}) corrosion potential, (I_{corr}) corrosion current densities, (βa) Tafel slope for an anode, (βc) Tafel slope for a cathode and IE% is the inhibition efficiency obtained from Eq (7).

$$IE\% = \frac{icorr - icorr'}{icorr} X\ 100 \qquad (7)$$

Where i_{corr} is the corrosion current densities of uninhibited mild steel and i_{corr}' is the corrosion current densities in the presence of the inhibitor. The values obtained from the Table (5), show as the concentration of the inhibitor increases the i_{corr} value decreases concerning i_{corr} value of the blank which has only SRB in

it. Higher i_{corr} value supports that the corrosion process is encouraged in the presence of bacterial species. The Tafel slope values for the anode and cathode decrease simultaneously indicating that it is a mixed type of inhibitor. The inhibitor is capable of ceasing the metal dissolution which is the anodic reaction and affecting the hydrogen evolution at the cathode, further affecting the H_2S evolution as HS^- is predominant than S^{2-} in bulk. Also suggests that this decrease in value is due to adsorption on the metal surface. The shift of E_{corr} values towards a more positive side as compared to uninhibited MS coupon suggests that the inhibitor is capable of obstructing both the anodic and cathodic reaction, but as the shift is on the positive side it is predominantly anodic type. As the concentration of inhibitor increases there is an increase in corrosion inhibition efficiency with maximum efficiency of 87.66% at 500 ppm concentration.[21]

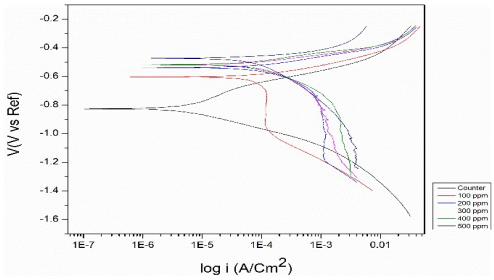

Fig.-7: Potentiodynamic Polarization Curves of MS in Barr's media inoculated SRB and with Varying Concentrations of N-((1H-benzo[d]1,2,3] traizol-1-yl) methyl)-4-chlorobenzenamine

Table-5: Parameters for the Bio-Corrosion of Mild steel in Barr's Media for 216hrs at R.T. Obtained from Potentiodynamic Polarization (PD)

S. No.	ppm	βa 10^{-3} (V/dec)	βc 10^{-3} (V/dec)	i_{corr} μA	$-E_{corr}$ mV	CR mpy	Inhibition Efficiency %
1	0	252	360	326	809	149.326	--
02	100	242	357	209	773	95.74	35.88
03	200	198	351	141	716	64.61	56.74
04	300	41.1	239	108	568	49.25	66.87
05	400	38.6	195	68.7	566	31.44	78.92
06	500	26.4	146	40.2	467	18.39	87.66

Surface Characterization

SEM Analysis

The surface morphology of MS coupons covered with inhibitory agents was studied with the help of SEM analysis. Fig 8(A), 8(B), and 8(C) are the SEM images of the MS coupons without inhibitor and with inhibitor, each inoculated with SRB in media respectively. Figure-8(A) image of MS without inhibitor, incubated for 216 hours at R.T with *Desulfovibrio desulfuricans* in Barr's media, shows the formation of pits on MS coupons. Figure-8(B) image of MS with 500 ppm concentration of inhibitor with *Desulfovibrio desulfuricans* in Barr's media shows the reduction in the formation of pits and the presence of cells on the surface respectively. Figure-8(C) shows an image of MS showing massive growth of bacteria on the surface of metal after 312 hours.[24]

EDAX Analysis

The surface composition of MS under study for bio-corrosion was analyzed using the EDAX technique. Figure-9(A) and 9(B) are the spectra obtained for metal coupons without inhibitor and with 500 ppm concentration of inhibitor after 312 hours. The images obtained, in Fig.-9(A) don't show the presence of a chloride peak, and a prominent peak was obtained for S which supports the formation of sulfides which is the bio-corrosion product. Figure-9(B) was detected with a chloride ion peak on the surface and the decrease of a sulfur peak supporting the above results, where adsorption of inhibitor molecule didn't allow the bacterial cells to attack the metal surface and protect it from bio-corrosion.[25]

The use of Heterocyclic organic compounds with substituted functional groups possesses good inhibitory action against corrosion. As per the literature, it is due to the conjugated system and the pi-electron-rich

property. Adsorption on a metal surface takes place due to a lone pair of electrons provided by heteroatom and vacant d-orbitals from the Fe atoms present on the surface which blocks the vacant site for corrosion reaction. It also depends on the size and electronegativity of the functional groups that an organic molecule bears.[26,27]

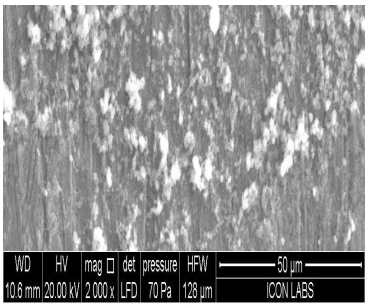

Fig.-8(A)

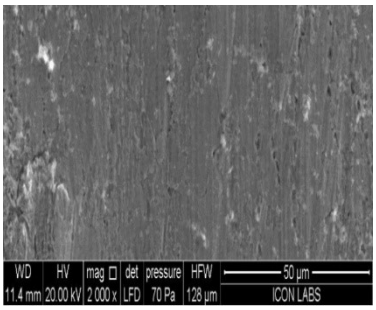

Fig.-8(B)

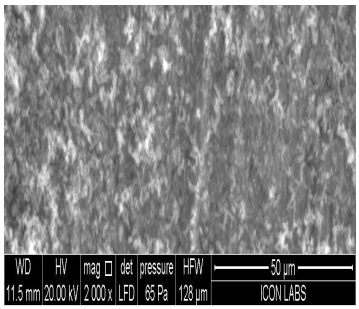

Fig.-8(C)

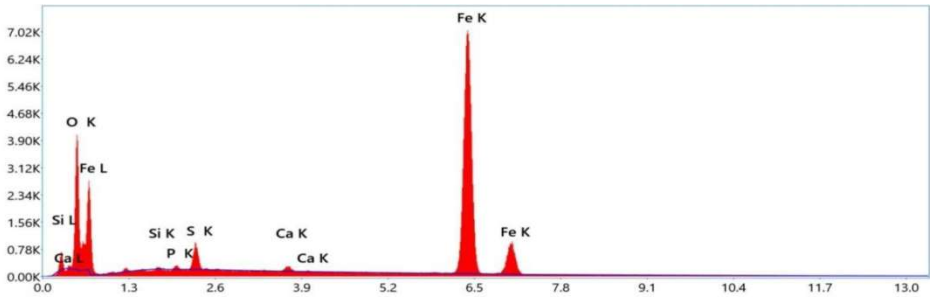

Fig.-9A: EDAX Analyzed Image of Polished Mild Steel Coupon Immersed in Barr's Media with *Desulfovibrio desulfuricans* for 216 hours

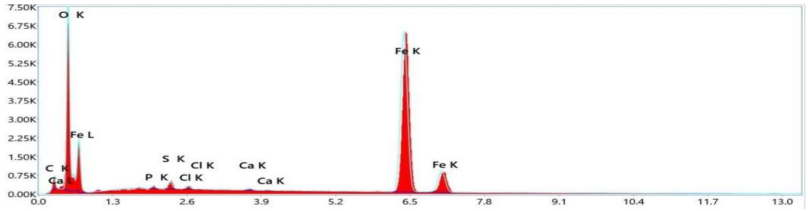

Fig.-9B: EDAX Analyzed Image of a Polished Mild Steel Coupon Immersed in Barr's Media Inoculated with *Desulfovibrio desulfuricans* and Inhibitor for 312 Hours

6. Mechanism of Inhibition

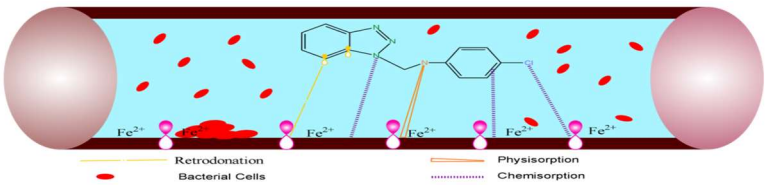

Fig.-10: Bio-corrosion inhibition mechanism

CONCLUSION

N-((1H-benzo[d]1,2,3] traizol-1-yl) methyl)-4-chlorobenzenamine, a benzotriazole and chloride derivative was synthesized with a 2-step reaction. The anti-bio-corrosive property of the synthesized organic compound was proved with results obtained from the gravimetric analysis, electrochemical techniques, and surface morphology analysis. Compiling the data obtained, the compound can be categorized into a mixed type of inhibitor, which acts spontaneously on the metal surface. As it obeys Langmuir adsorption isotherms it supports the formation of a monolayer of inhibitor on metal surface. The adsorption on the MS surface is detected by SEM and EDAX images which indicate that adsorption has taken place on the MS surface.

ACKNOWLEDGMENTS
Authors are grateful to the authorities of their institutions for their cooperation and support.

CONFLICT OF INTERESTS
The authors declare that there is no conflict of interest.

AUTHOR CONTRIBUTIONS
All the authors contributed significantly to this manuscript, participated in reviewing / editing, and approved the final draft for publication. The research profile of the authors can be verified from their ORCID ids, given below:

Dhanali Shah https://orcid.org/0009-0001-9083-1881
R. S. Dubey https://orcid.org/0009-0002-3803-1075

Open Access: This article is distributed under the terms of the Creative Commons Attribution 4.0 International License (http://creativecommons.org/licenses/by/4.0/), which permits unrestricted use, distribution, and reproduction in any medium, provided you give appropriate credit to the original author(s) and the source, provide a link to the Creative Commons license, and indicate if changes were made.

REFERENCES
1. J. Li, E. Zhou, F. Xie, Z. Li, F. Wang, and D. Xu, *Corrosion Science,* **243,** 112593(2025), https://doi.org/10.1016/j.corsci.2024.112593
2. L. Wang, J. Li, F. Xie, D. Wang, and M. Wu, *Journal of Electroanalytical Chemistry*, **973,** 118707(2024), https://doi.org/10.1016/j.jelechem.2024.118705
3. R. Javaherdashti, Microbiologically Influenced Corrosion, An Engineering Insight-(Engineering materials and processes), Springer-Verlag London Limited, p.90,123, (2008).
4. M. Sun, X. Wang, and W. Cui, *Measurement: Sensors*, **34,** 101266(2024), https://doi.org/10.1016/j.measen.2024.101266
5. T. Rao, T. Sairam, B. Viswanathan, and K. Nair , *Corrosion Science*, **42**,1417(2000), https://doi.org/10.1016/s0010-938x(99)00141-9
6. A. Singh, C. Sharma, and S. Lata, *Anti-Corrosion Methods and Materials*, **58**, 315(2011), https://doi.org/10.1108/00035591111178873
7. I. T. Fonseca, M. Feio, A. R. Lino, M.Reis, and V. L. Rainha, *ElectrochimicaActa*, **43**, 213(1998), https://doi.org/10.1016/s0013-4686(97)00227-2
8. X. Liu, Y. Wang, Y. Song, W. Liu, J. Zhang, N. Li, K. Dong, Y. Cai and E. H. Han, *Corrosion Science,* **240,** 112479(2024), https://doi.org/10.1016/j.corsci.2024.112479
9. K. M. Shwetha, B. M. Praveen and B. K. Devendra, *Results in Surfaces and Interfaces*, **16,** 100258(2024), https://doi.org/10.1016/j.rsurfi.2024.100258
10. R. Aslam, M. Mobin, S. Zehra and J. Alsam, *Journal of Molecular Liquids,* **364,** 119992(2022), https://doi.org/10.1016/j.molliq.2022.119992
11. R. Jia, J. L. Tan, P. Jin, D. J. Blackwood, D. Xu, and T.Gu, *Corrosion Science*, **130**, 1(2018), https://doi.org/10.1016/j.corsci.2017.10.023
12. N. P. Swathi, S. Samshuddin, T. A. Aljohani, K. Rasheeda, V. D. Alva, F. Y.Alomari, and A. H. Alamri, *Materials Chemistry and Physics*, **291**, 126677(2022), https://doi.org/10.1016/j.matchemphys.2022.126677
13. H. Lu, X. Ji, X. Ci, H. Zhu, Q. Wang, Y. Zong, and H. Tian, *Colloids and Surfaces a Physicochemical and Engineering Aspects*, **674**,131892(2023), https://doi.org/10.1016/j.colsurfa.2023.131892
14. L. K. Soni, Ph. D. Thesis, Department School of Pharmacy, University of Devi Ahilya Vishwavidyalaya, Indore, Madhya Pradesh, India, (2016), http://hdl.handle.net/10603/241465
15. H. U. Nwankwo, L. O. Olasunkanmi, and E. E. Ebenso, *Journal of Bio- and Tribo-Corrosion*, **4**, (2018), https://doi.org/10.1007/s40735-018-0130-7
16. H. U. Nwankwo, E. D. Akpan, L. O. Olasunkanmi, C. Verma, A. M. Al-Mohaimeed, D. A. A. Farraj, and E. E. Ebenso, *Journal of Molecular Structure*, **1223**, 129328(2021), https://doi.org/10.1016/j.molstruc.2020.129328

17. B. Pang, H. Li, C. Ding, C. Song, and S. Wang, *Frontiers in Materials*, **11**, (2024), https://doi.org/10.3389/fmats.2024.1390242
18. D. R.Gusti, N. Nelson, I. Lestari, P. Ramadhanti, and R. G. Sibarani, *Jurnal Ilmiah Berkala: Sains dan Terapan Kimia*, **17**, 11(2023), https://doi.org/10.20527/jstk.v17i1.9150
19. N. D. Kalisa, T. Muhizi, J. J. Y. Niyotwizera, J. B. Barutwanayo, and J. B. Nkuranga, *Rwanda Journal of Engineering Science Technology and Environment*, **3(1)**, (2020),https://doi.org/10.4314/rjeste.v3i1.10
20. M. A. Adebayo, S. O. Akande, A. D. Olorunfemi, O. O. Ajayi, J. I. Orege, and E. F. Daniel, *Progress in Chemical and Biochemical Research*, **4(1)**, 80(2021), https://doi.org/10.22034/pcbr.2021.120449
21. B. Gao, X. Zhang, and Y. Sheng, *Materials Chemistry and Physics*, **108(2–3),** 375(2008), https://doi.org/10.1016/j.matchemphys.2007.10.033
22. O. S. I. Fayomi, and I. G. Akande, *Journal of Bio- and Tribo-Corrosion*, **5(1)**, Article 23 (2019), https://doi.org/10.1007/s40735-018-0214-4
23. B. Shyamvarnan, S. Shanmugapriya, J. A. Selvi, P. Kamaraj, and R. Mohankumar, *Materials Today Proceedings*, **40**, S192(2021),https://doi.org/10.1016/j.matpr.2020.09.085
24. P. Kamble, R. S. Dubey, *International Journal of Scientific Research in Science, Engineering and Technology*, **5(4)**, 95(2018).
25. I. N. Etim, J. Dong, J. Wei, C. Nan, D. B. Pokharel, A. J. Umoh, D. Xu, M. Su, and W. Ke, *Journal of Material Science and Technology*, **64**, 126(2021), https://doi.org/10.1016/j.jmst.2019.10.006
26. S. Chen, K. Zhao, and G. Chen, *Journal of Chemistry*, (2015), https://doi.org/10.1155/2015/201259
27. E. E. El-Katori, R. A. El-Saeed, and M. M. Abdou, *Arabian Journal of Chemistry*, **15(12)**, 104373(2022), https://doi.org/10.1016/j.arabjc.2022.104373

[RJC-9178/2024]